Climate Dynamics
https://doi.org/10.1007/s00382-018-4214-3

Projected change in characteristics of near surface temperature inversions for southeast Australia

Fei Ji[1] · Jason Peter Evans[2] · Alejandro Di Luca[2] · Ningbo Jiang[1] · Roman Olson[3] · Lluis Fita[4] · Daniel Argüeso[5] · Lisa T.-C. Chang[1] · Yvonne Scorgie[1] · Matt Riley[1]

Received: 26 October 2017 / Accepted: 6 April 2018

Abstract
Air pollution has significant impacts on human health. Temperature inversions, especially near surface temperature inversions, can amplify air pollution by preventing convective movements and trapping pollutants close to the ground, thus decreasing air quality and increasing health issues. This effect of temperature inversions implies that trends in their frequency, strength and duration can have important implications for air quality. In this study, we evaluate the ability of three reanalysis-driven high-resolution regional climate model (RCM) simulations to represent near surface inversions at 9 sounding sites in southeast Australia. Then we use outputs of 12 historical and future RCM simulations (each with three time periods: 1990–2009, 2020–2039, and 2060–2079) from the NSW/ACT (New South Wales/Australian Capital Territory) Regional Climate Modelling (NARCliM) project to investigate changes in near surface temperature inversions. The results show that there is a substantial increase in the strength of near surface temperature inversions over southeast Australia which suggests that future inversions may intensify poor air quality events. Near surface inversions and their future changes have clear seasonal and diurnal variations. The largest differences between simulations are associated with the driving GCMs, suggesting that the large-scale circulation plays a dominant role in near surface inversion strengths.

Keywords Temperature inversion · NARCliM · Ensemble mean · Near surface inversion

1 Introduction

Population growth, urbanization and increasing demands for transportation and energy consumption are ongoing challenges to impact our air quality, especially in large cities (Bei et al. 2016a; Wang et al. 2016; Feng et al. 2014). Air pollution has substantial impact on human health (Chen et al. 2016; Zora et al. 2013; Abdul-Wahab et al. 2005). It has been estimated that each year more than 3000 premature deaths in Australia are linked to urban air pollution (AIHW 2007) even though Australia has very clean air by world standards.

Air pollution is undoubtedly caused by anthropogenic emissions of gas and particulates. However, high pollution episodes are often consistent with the expected effects of low-level temperature inversions (VanReken et al. 2017; Bei et al. 2016b; Hou and Wu 2016; Czarnecka et al. 2016; Wang et al. 2015; Whiteman et al. 2014; Feng et al. 2014). Pollution levels usually increase as the inversion strengthens (Devasthale and Thomas 2012; Wallace et al. 2010), and worse pollution episodes are often associated with persistent inversions (Largeron and Staquet 2016; Bei et al. 2016a). Warm air above cooler air acts like a lid, suppressing vertical mixing and trapping the cooler air near the surface. As pollutants from vehicles, fireplaces, and industry are

Electronic supplementary material The online version of this article (https://doi.org/10.1007/s00382-018-4214-3) contains supplementary material, which is available to authorized users.

✉ Fei Ji
fei.ji@environment.nsw.gov.au

[1] NSW Office of Environment and Heritage, Sydney, Australia

[2] Climate Change Research Centre and ARC Centre of Excellence for Climate Extremes, University of New South Wales, Sydney, Australia

[3] Yonsei University, Seoul, Republic of Korea

[4] Laboratoire de Météorologie Dynamique, CNRS, Université Pierre et Marie Curie, Paris, France

[5] Department of Physics, University of Balearic Islands, Palma de Mallorca, Spain

Published online: 08 May 2018

emitted into the air, the inversion traps these pollutants near the ground, leading to poor air quality.

Temperature inversions can be classified into diverse types based on their formation mechanisms such as radiative inversions, marine inversions, frontal inversions, subsidence inversions, and valley inversions. Radiative inversions are a common inversion over inland areas where radiation at the land surface is more efficient than the air, this results in the colder air lying near the ground with warmer air above during the night. Marine inversions are common for coastal areas where cool ocean air is blown inland under the warmer air that is over land. Frontal and subsidence inversions are caused by some specific weather systems. Valley inversions are a kind of radiation inversion which occurs over valleys and hilly areas. No matter which kind of inversion, only those with bases near the Earth's surface (near surface inversions) have major impacts on air quality as they can lead to pollution being trapped close to the ground, with possible adverse effects on health (Rendón et al. 2014; Beard et al. 2012).

Evolution of temperature inversions and their characteristics were discussed in several studies (Kahl et al. 1990, 1992; Connolley 1996; Whiteman et al. 1999). These studies found that inversion evolution is primarily forced by synoptic-scale events in winter, however, in other seasons, the radiation-induced nocturnal inversion is destroyed nearly every day by the daytime growth of convective boundary layers. Bailey et al. (2011), and Milionis and Davies (2008) investigated the relation between temperature inversions and ambient atmospheric circulation. They found that temperature inversions are sensitive to the larger scale circulations, however, local factors (location, topography, etc) might overwhelm the synoptic conditions, especially for coastal regions. Conditions that favour the development of a temperature inversion are calm winds, clear skies, and long nights.

Seasonal and long-term variations of temperature inversions recently attracted research interest due to their adverse impacts on air quality and human health (Kassomenos and Koletsis 2005; Nodzu et al. 2006; Bourne et al. 2010; Pietroni et al. 2014). However, these climatological studies do not allow the exploration of future projections because they are based only on observations (station sounding or remote sensing data).

Climate change will affect the surface energy balance and synoptic-scale dynamics. Changes in weather factors such as surface temperature, humidity and wind, and synoptic types will dynamically influence local weather conditions which are associated with temperature inversions. For example, all other conditions being the same, lower humidity and lighter wind would favor the development radiative inversions (Bailey et al. 2011).

With global warming and on-going pressure on air quality, there is growing interest in the relationship between global warming and local inversions. Caserini et al. (2017) used one global climate model (GCM) to assess influence of climate change on the frequency of day-time temperature inversion in the Po Valley, Italy. Their results projected 10% increases in day-time inversions for late twenty-first century. Ji et al. (2015) assessed the impact of climate changes on temperature inversions using the NARCliM outputs (Evans et al. 2014) for all inversions below 500 hPa. Their results projected diverse changes in frequency, intensity and duration of temperature inversion for different areas in southeast Australia. For the northern land areas little change in frequency and duration are projected but with large decrease in intensity, however larger increase in frequency and duration are projected for the southern land areas but their intensity are projected to slightly decrease.

In this study, we build on Ji et al. (2015) to focus on near surface inversions (those with a base below 200 m), which can result in major air quality impacts, to analyze their future changes. First we evaluate the NARCliM simulations' capability to capture near surface inversions, then we analyze future changes in seasonal and diurnal characteristics of near surface inversions and compare the results with those for all inversions presented in Ji et al. (2015). Finally, we analyze the significance and model agreement of the future changes in near surface inversions.

2 Data

2.1 Observed temperature profiles

There are 9 weather stations (Brisbane, Moree, Cobar, Williamstown, Sydney, Wagga Wagga, Adelaide, Mt Gambier, and Melbourne) within the NARCliM domain (Table 1) that provide observations of vertical temperature profile (http://slash.dotat.org/atmos/info.html). We have collected vertical temperature profiles for all stations starting from Feb 2002 to date. The temperature profiles are mostly recorded at 11UTC (local time 9 pm) and 23UTC (local time 9 am) for all stations except for Sydney where temperature profiles are recorded at 4UTC (local time 2 pm) and 19UTC (local time 5 am). There are about 340 day-time temperature profiles in a year for all stations, however, only Brisbane, Sydney, Adelaide and Melbourne have similar number of night-time temperature profiles in a year. Cobar and Moree have about 150 and 130 night-time temperature profiles a year, respectively, Wagga Wagga and Mt Gambier 40 night-time temperature profiles, and Williamstown only 6 night-time temperature profiles in a year (Table 1). Moree, Cobar and Wagga Wagga are inland towns, Mt Gambier is about 50 km from the sea, and others are all coastal cities (Fig. 1).

Table 1 Location of observation stations and number of recorded temperature profiles

Station	Latitude	Longitude	Elevation (m)	Number of temperature profile at 9 am (local time)	Number of temperature profile at 9 pm (local time)
Brisbane	− 27.3833	153.1166	4	335	355
Moree	− 29.4666	149.8500	212	340	127
Cobar	− 31.4833	145.8333	264	338	150
Williamtown	− 32.8000	151.8333	9	337	6
Sydney	− 33.9333	151.1666	6	347[a]	356[a]
Wagga	− 35.1666	147.4666	221	344	42
Adelaide	− 34.9500	138.5332	6	323	353
Mt Gambier	− 37.6833	144.8500	63	347	43
Melbourne	− 37.7500	140.7833	132	335	356

[a]Temperature profiles are collected at 5 am and 2 pm for Sydney

2.2 Simulated temperature profiles

The simulated temperature profiles are derived from the NARCliM project (Evans et al. 2014). The project provides vertical temperature profiles every 3-h for each 10 km by 10 km grid cell in the NARCliM domain (Fig. 1), which can be used to detect temperature inversions and investigate their future changes. Within the NARCliM domain, the Great Dividing Range (the most substantial mountain range in Australia) stretches thousands of kilometers from Queensland, running the entire length of the eastern coastline through NSW, and then into Victoria. The mountain range runs almost north–south, intercepting the prevailing westerly winds in winter and the easterly winds in summer, and acting as a major climatic barrier separating southeast Australia into distinct climate zones. Flinders Rangers in South Australia also influences the regional climate.

In NARCliM, simulations from four GCMs were used to drive three regional climate models (RCMs) to form a 12 member GCM/RCM ensemble. The four GCMs are MIROC3.2, ECHAM5, CCCMA3.1, and CSIRO-MK3.0 from the CMIP3 ensemble, which were selected based on model performance over Australia, independence of errors, and to span the full range of potential future climates over south-eastern Australia (Evans et al. 2014). The three RCMs (Table 2) correspond to three different physics scheme combinations of the WRF V3.3 model (Skamarock et al. 2008), which were also chosen for adequate skill and error independence, following a comprehensive analysis of 36 different combinations of physics parametrizations over eight significant East Coast Lows (ECLs) (Evans et al. 2012; Ji et al. 2014). For the selected three RCMs, the WRF Double Moment 5-class (WDM5) microphysics scheme and NOAH land surface scheme are used in all cases, with cumulus physics using either the Kain–Fritsch (KF) or Betts–Miller–Janjic (BMJ) scheme. Planetary boundary layer (PBL) and surface physics use either the Yonsei University PBL scheme with the MM5 similarity theory surface layer scheme (YSU/MM5) or the Mellor–Yamada–Janjic PBL scheme with the Eta similarity theory surface layer (MYJ/Eta). The two radiation physics schemes use either the NCAR Community Atmosphere Model scheme (CAM) for both longwave and shortwave radiation, or a combination of the Rapid Radiative Transfer Model for longwave radiation with the Dudhia shortwave scheme (RRTM/Dudhia). For more information on the specifics of the model parameters see Skamarock et al. (2008). Sub-grid scale processes in the urban environment were described using the Single-Layer Urban Canopy Model [SLUCM (Kusaka et al. 2001)]. The SLUCM uses a tiling approach, where the surface energy budget is calculated separately for both impervious and vegetated cover. These are provided to the atmospheric model according to the percentage of each surface that compose the urban tile, which in this case was set to high-density residential (10% is covered by vegetation). Each grid point is assigned a single land cover category, either urban or one of the natural landscapes.

The resultant ensemble improves substantially on the GCMs in the simulation of Australian mean and extreme climate (Evans et al. 2013; Olson et al. 2016). By explicitly using model independence it is possible to create relatively small ensembles that are able to reproduce the ensemble mean and variance from the large parent ensemble as well as minimize the overall error (Evans et al. 2013a). The outputs within the NARCliM domain (Fig. 1) are used in the study. The results over land areas are discussed in the text.

For quantifying RCMs performance, the three RCMs are also driven by NCEP reanalysis (Kalnay et al. 1996) from 1950 to 2009. For the future projections the SRES A2 emission scenario is used. Each RCM-GCM pair has been run for three 20-year periods: 1990–2009, 2020–2039, and 2060–2079.

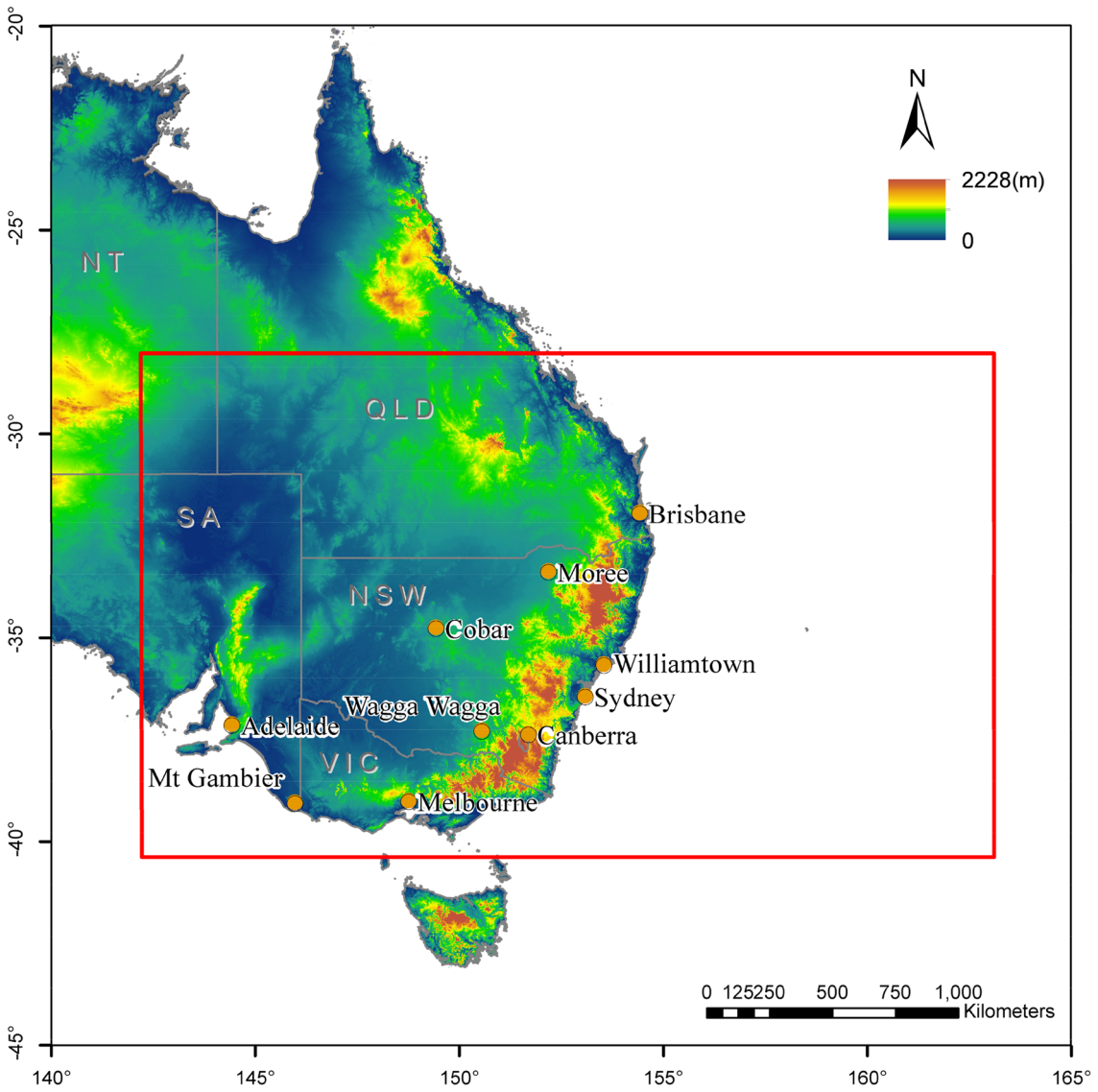

Fig. 1 Map showing WRF model domain with grid spacing of about 10 km (NARCliM domain shown with red outline). QLD, NSW, VIC, SA and NT are initial of Queensland, New South Wales, Victoria, South Australia and Northern Territory, which are Australia's states. Nine of ten locations except for Canberra are sites where sounding data are recorded. Sydney, Melbourne, Brisbane, Adelaide and Canberra are capital cities

Table 2 Three selected WRF physics scheme combinations

Ensemble member	Planetary boundary layer physics/surface layer physics	Cumulus physics	Shortwave/longwave radiation physics
R1	MYJ/Eta similarity	KF	Dudhia/RRTM
R2	MYJ/Eta similarity	BMJ	Dudhia/RRTM
R3	YSU/MM5 similarity	KF	CAM/CAM

Previous evaluation of NARCliM simulations shows that RCMs have strong skill in simulating the precipitation and surface temperature for Southeast Australia with a small cold bias, and overestimation of precipitation along the Great Dividing Range (Evans et al. 2013b, 2016; Ji et al. 2016; Olson et al. 2016). The differing responses of the RCMs confirm the utility of considering model independence when choosing the RCMs. The RCM response

to large scale modes of variability also reflects the observations well (Fita et al. 2016). Through these evaluations no major deficiencies are found in the experiments that prevent their use for climate applications while there is a spread in model predictions, with no single model performing the best for all variables and metrics. The use of the full ensemble provides a measure of robustness such that any result that is common through all models in the ensemble is considered to have higher confidence.

For easier description in this paper, the simulations driven by the same GCM are referred to as "same GCM driven simulations", the simulations using the same RCM are referred to as "same RCM used simulations". In total, there were 4 "same GCM driven simulations" (average of three members) and 3 "same RCM used simulations" (average of four members).

3 Methodology

3.1 Evaluation of near surface inversions

The evaluation is undertaken for near surface inversions in recent temperature profiles (2002–2009 for 9 stations). On average, there are 10 and 3 measurements that are below 1500 and 200 m, respectively in the observed temperature profiles. The vertical resolution is good enough to detect near surface inversions from the original temperature profiles.

The simulated temperature profiles from the NCEP reanalysis driven simulations (Evans et al. 2014) from 2002 to 2009 are used to detect inversions (as described in Sect. 3.2). On average, there are 12 and 3 vertical levels in WRF simulations that are below 1500 and 200 m, respectively. So simulations have a similar vertical resolution to observations in the lower troposphere. The inversion frequency and strength at the nearest neighbor WRF grid points are used to compare with observed inversion frequency and strength at each site. The observed temperature profiles are recorded at 4 UTC and 19UTC for the Sydney station and 11 UTC and 23 UTC for other stations, however, the simulated temperature profiles are available at 3-hourly intervals starting at 00 UTC. We identify simulated near surface inversions at 12 UTC and 00 UTC, and compare with the observed near surface inversions at 11UTC and 23 UTC for all stations except for Sydney where simulated near surface inversions at 3 UTC and 18 UTC are compared with observed near surface inversions at 4 UTC and 19 UTC respectively. As there are only two measurements a day in the observation, we can only evaluate frequency and strength of inversions at the two measurement times.

3.2 Identification of temperature inversion

According to the definition, a temperature inversion is a thin layer of the atmosphere where temperature increases with altitude. For each grid point within the NARCliM domain and for each time interval in the output, the temperature profile below 500 hPa is checked to detect low level temperature inversions by comparing the temperature at each level with that at the level below. A temperature inversion is identified when the temperature differences between the two levels is larger than zero. As the near surface inversions have larger air quality impacts, only the lowest level inversion is kept for further analyses if there are multiple inversions identified in one temperature profile. We record temperature inversion parameters (temperature, height, pressure at the top and base of the inversion layer) and analyze the probability density function (pdf) of base height of indicated temperature inversions, the results show that there are more than 60% of inversions with base height less than 200 m above the ground for land areas. In this study, we refer to these inversions as "near surface inversions" and extract them to analyze present conditions and future changes of near surface inversion characteristics. Inversion parameters of interest include inversion base height, inversion depth, temperature difference between the top and base of the inversion layer, duration, and strength which is defined as the temperature difference over the inversion depth (dT/dZ).

Frequency of temperature inversion is calculated as the number of times with a temperature inversion divided by the total number of output time steps. The mean duration of a temperature inversion is calculated by the accumulated duration for all temperature inversions divided by the number of temperature inversions.

In this study, we focus on three near surface inversion characteristics: frequency, strength and duration.

3.3 Examination of temperature inversion characteristics

The frequency, strength and duration for each grid within the NARCliM domain are calculated for each of 12 NARCliM ensemble members, for each of three time periods. The changes in variables of interest are the difference between that for future time periods (2020–2039, 2060–2079) and the historical period (1990–2009). The relative change is defined as (future − present)/present × 100. The results for each ensemble member are averaged to get the ensemble mean.

As shown in Ji et al. (2015), future changes in inversion characteristics are generally much smaller for 2020–2039 (near future) than 2060–2079 (far future). This is expected as climate change signal will be stronger by the end of the

century. In this paper, we therefore focus on far future to analyze changes in characteristics of near surface inversions.

The ensemble mean and change of inversion characteristics for "Same GCM driven simulations" and "Same RCM used simulations" are calculated to discuss the differences in projections between "Same GCM driven simulations" and "Same RCM used simulations" respectively.

There are five state capital cities (Adelaide, Brisbane, Canberra, Melbourne and Sydney) within the NARCliM domain (Fig. 1). The ensemble mean at these cities is extracted to analyze diurnal variation of inversion characteristics and their future changes.

3.4 Significance and model agreement of the changes

The significance of changes of individual simulation was estimated with respect to the inter-annual variability using a Students t-test at the 5% significance level ($p < 0.05$) assuming equal variances for the past and future simulated time series. The use of t-tests essentially assumes that annual mean values follow a normal distribution in past and future periods.

We present the results on significance into three categories generally following Tebaldi et al. (2011): significant agreeing areas (stippled), insignificant areas (shown in color), and significant disagreeing areas (shown in grey). In significant agreeing areas, at least half of models show a significant change (5% significance with t test) and at least 80% of significant models agree on the direction of change. We consider these changes to be robust within the ensemble. In insignificant areas, less than half of the models show significant changes. These are areas where the ensemble is projecting little change. In significant disagreeing areas, at least half of the models show a significant change, but less than 80% of significant models agree on the direction of the change. In these areas we have low confidence in the projected changes.

4 Results

4.1 Evaluation of temperature inversions

The frequency and strength of near surface inversions at 9 stations have been compared between simulations and observations from February 2002 to December 2009. The results are summarized in the Fig. 2. The day-time inversions are evaluated at all 9 stations; however, the night-time inversions are only evaluated at 4 stations (Brisbane, Sydney, Adelaide and Melbourne) as there are not enough temperature profiles for other stations.

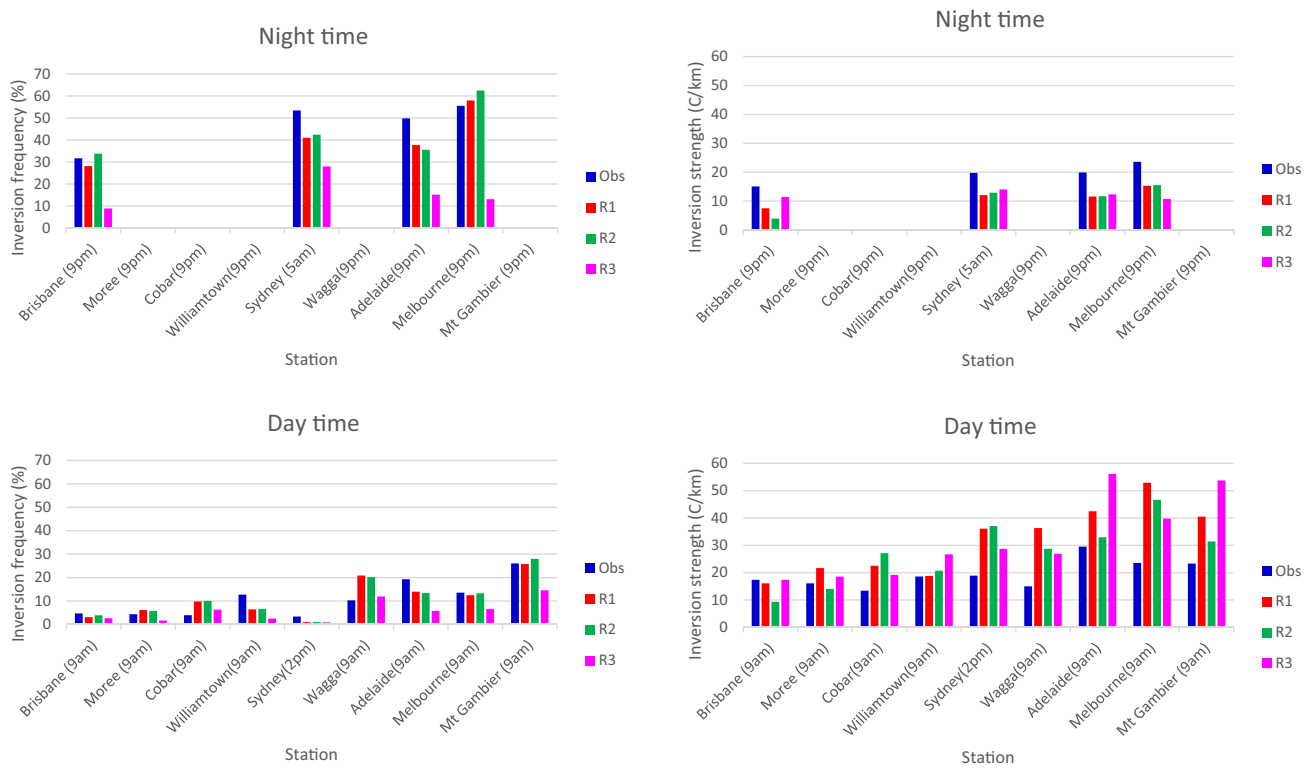

Fig. 2 Day-time and night-time frequency and strength of near surface inversions for monitoring stations

1. Frequency

There is more than 50% chance of a near surface inversion at night for Sydney and Melbourne, and about 50% and 30% chance for Adelaide and Brisbane respectively. This is generally captured by R1 and R2 simulations even if there are some under-estimations for Sydney and Adelaide. The mean relative bias between simulation and observations for these four stations is about 16 and 21% for R1 and R2 simulations individually. However, about 70% relative bias for R3 simulations. During day time, all stations have fewer near surface inversions. Mt Gambier has about 25% chance to have day-time inversion which is well simulated by R1 and R2 simulations with less than 10% relative bias, but about 40% relative bias for R3 simulations. Williamstown, Adelaide and Melbourne have 10–20% chance to have a day-time near surface inversion, which is generally captured by R1 and R2 simulations with 28 and 46% relative bias respectively, but more than 100% relative bias for R3 simulation. The rest of the stations have less than 10% chance to have a day-time near surface inversion, which is captured by R1 and R2 simulations. In general, R1 and R2 simulations can simulate the frequency of near surface inversion well, however, R3 simulations generally under-estimate day-time and night-time near surface inversions for all stations. Overall there is higher likelihood of night-time near surface inversions which is captured by all simulations including R3.

R3 has the same physical parameterization combination as R1 except for the planetary boundary layer (PBL) and radiation parameterizations (Table 2). Radiation parameterization is important in simulating energy balance. Surface temperature is better simulated in R3 comparing to R1 and R2 with smaller biases which indicated that CAM/CAM radiation scheme used in R3 accurately simulate energy balance on the surface (Ji et al. 2016). However, near surface temperature inversion is poorly simulated in R3. This is due to unrealistic simulated mixing process within the PBL. YSU, used in R3, is non-local PBL scheme in which a deeper layer covering multiple levels is mixed vertically. MYJ, used in R1, is a local PBL scheme in which vertical mixing is only considered in immediately adjacent vertical levels. Therefore, Low-level lapse rates are typically steeper for non-local than local schemes (Cohen et al. 2015). It gets harder to form an inversion during the night and easier to break up an inversion during day, due to deeper mixing process in non-local schemes. This is the main cause of the under-estimation of near surface inversions by R3.

2. Strength

In observations, there is not much difference in strength between day-time and night-time near surface inversions for all 4 stations (about 20 °C/km) except for Adelaide where day-time inversions are stronger (about 30 °C/km). However, all three simulations generally underestimate/overestimate the strength of night-time/day-time near surface inversions. Biases in strength for day-time inversions are generally larger than night-time inversions. The strength of day-time inversions in Brisbane, Moree and Williamstown is well captured by simulations, relative biases are under 30%. The larger overestimation can be observed in Melbourne, Mt Gambier and Cobar where the maximum biases can be more than 100%. The mean relative bias in strength for all stations are about 60% for R1 simulations, 50% for R2 simulations, and 55% for R3 simulations.

Larger bias in strength for day-time inversions might be due to only a few near surface inversions during day-time as such the average inversion strength is very sensitive to each inversion event. Any bias in the estimation of inversion events might have larger impact on the average strength. There is 1 h gap between simulation and observation. This could be another reason for overestimation in strength during day time and under-estimation in strength during night time, as inversions generally get stronger during night and weaker after sunrise.

4.2 Mean and changes in near surface inversions

Frequency, strength and duration are three key characteristics for an inversion. The present mean and future changes in three characteristics of near surface inversions are presented in Fig. 3.

1. Frequency

For daily average, a weak gradient of the frequency of near surface inversions can be observed for land areas for the period of 1990–2009 (the top left panel in Fig. 3). There are slightly higher values (44–48%) over the inland areas and relatively lower frequency over the Great Dividing Range (32–36%) and Flinders Rangers in South Australia. It is almost uniform in values for majority of domain that is around 40–44%. Near surface inversion frequency is projected to have a 0–10% relative increase over the southern land areas and a 0–10% relative decrease over the northern land areas (the top right panel in Fig. 3). The projected changes in near surface inversion frequency are significant agreeing over some inland areas (most of which see a decrease). However, the changes in frequency are not significant for coastal land areas though the relative changes are larger over these areas.

When compared with Fig. 1 in Ji et al. 2015, more than 60% of inversions are near surface inversions over land areas. Similar changes in frequency are projected for near surface inversions and all inversions over land areas.

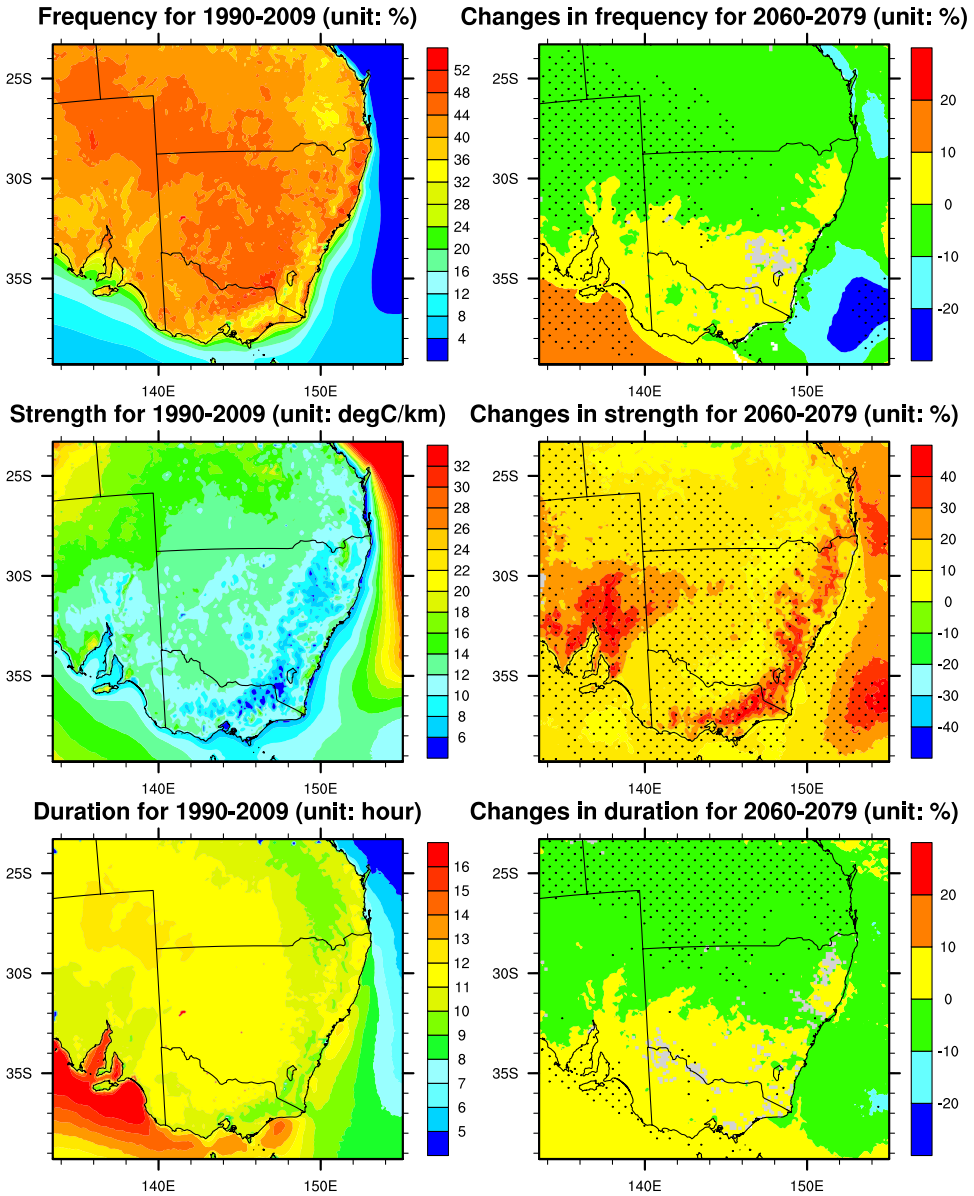

Fig. 3 Mean near surface inversions and changes in near surface inversions for 2060–2079 relative to 1990–2009. Stippled (significant agreeing) areas indicate that half or more models show statistically significant change, with 80% or more of the significant models changed in the same direction. Grey (significant disagreeing) areas indicate that half or more models show statistically significant change, with less than 80% of significant models changed in the same direction

Near surface inversions have a clear diurnal circle with more than 70% of days with inversions at night for most land areas and less than 10% of days with inversions during day time (Fig S1). Near surface inversion begin to breakup after the sunrise and form after the sunset. They mostly occur in the early morning and least occur in the afternoon except over water bodies (lakes and reservoirs). There are some differences in inversion frequency between the eastern and western domains during the sunrise or sunset periods. There are fewer inversions for the eastern domain than the western domain after the sunrise, however after the sunset, the pattern is opposite. This implies most near surface inversions are radiative inversions which have a clear diurnal cycle.

Frequency of near surface inversion is projected less than 10% increase/decrease for the southern/northern land domain for night time. However more than 30% increase in frequency is projected during day time especially in the afternoon (Fig S2). The large magnitude of relative changes in frequency is due to low frequency during day time for the 1990–2009 period. This indicates there is little change in near surface frequency at night but there will be more near surface inversions during day time in the future, even if these changes are mostly not significant. More day-time inversion will imply more adverse air quality impacts during daytime.

2. Strength

For daily average, a northwest-southeast strength gradient can be observed with 8–12 °C/km over coast areas, 12–16 °C/km over central west areas, and more than 20 °C/

km over far west areas (the central left panel in Fig. 3). Increase in strength is projected over almost all land areas, especially for the Great Dividing Range and Flinders Rangers in South Australia where more than 30% increase in strength is projected (the central right panel in Fig. 3). Changes in strength are statistically significant for most land areas where more than 10% increase in strength is projected.

When compared with Fig. 2 in Ji et al. 2015, near surface inversions are much stronger than all inversions (central panels in Fig. 3). Contrasting to projections for near surface inversions, 10–15% decrease in intensity is projected for the northern domain, a 0–5% increase for the southern domain, and 5–10% increase for Great Dividing Range and Flinders Rangers for all inversions.

The diurnal variation of near surface inversion strength is shown in Fig S3. Just after the sunset, inversion strength is the lowest and increases slowly during night. After sunrise, most inversions break-up (Fig S1), however the remaining inversions are usually very strong (above 20 °C/km for northwestern and coastal areas). For future, less than 20% increase/decrease in strength is projected for southern/northern land areas for night time inversion, however, more than 40% increase in strength is projected for day time inversion especially for coastal and high topography areas where more than 80% increase in strength is projected (Fig S4).

3. Duration

There is not much variation in duration for near surface inversions over land areas (bottom panel in Fig. 3). 9–11 h for inversions over high topography areas along Great Dividing Range and Flinders Rangers in South Australian, extending up to 12–13 h for the remaining land areas. This reflects most near surface inversions that form after the sunset and break up after the sunrise.

A 0–10% decrease in duration of near surface inversion is projected for the northern land areas, and a 0–10% increase for the southern land areas. Changes in duration are mostly significant agreeing for northern land areas.

The mean duration for near surface inversions is smaller than that for all inversions (Fig. 3 in Ji et al. 2015). Changes in duration for near surface inversions are not as large as those for all inversions over southern land areas.

All these results project a small increase/decrease frequency and duration for southern/northern land areas, however a larger increase in strength is projected for the whole land domain especially for the Great Dividing Range and Flinders Rangers in South Australia.

4.3 Seasonal variation of near surface inversions

A clear seasonal variation in near surface inversion frequency can be observed with more near surface inversions in winter (50–60%) and fewer inversions in summer (30–40%). Small changes are projected for all seasons except for winter (JJA) when significant decreases are projected for some areas (Fig S5).

There is a clear seasonal variation in strength of near surface inversions over land areas with the strongest inversions (above 28 °C/km) in summer over the southern land areas, in winter over the northern domain and in other seasons over the western domain (Fig. 4). The changes in strength are significant largely for larger increases in most land areas in winter and spring, other significant increases in strength occur in scattered grids in southern areas in summer and autumn.

Near surface inversions over the coastal areas do not change much in duration across seasons, but those over inland areas have a strong seasonal variation with the longest duration (14–16 h) in winter and the shortest duration (8–10 h) in summer (Fig S6). The changes in duration are significant largely for small decreases in northern land areas for all seasons, and small increases in duration in southern land areas in spring.

4.4 Diurnal variation of near surface inversions

Near surface inversions over the five capital cities have a clear diurnal cycle (Table 3). There is more than 40% chance of a near surface inversion during night, reducing to less than 10% in the late morning and few near surface inversions in the afternoon. The differences between cities are minor when compared with their diurnal variations. The correct representation of the diurnal cycle of the inversions done by the model is complimentary proof of the skill of the model.

Smaller changes are projected for inversion frequency for each city except for Adelaide where more than 20% changes are projected for afternoon. However, these changes are not statistically significant.

An apparent diurnal cycle of inversion strength is presented in all five capital cities as well (Table 4), with stronger inversions during day (20–80 °C/km) and weaker inversions during night (less than 10 °C/km). So, while few near surface inversions occur during day time, when they do they are usually very strong. About 10% increase in strength is projected for all cities during night time except for Brisbane where a minor decrease (less than 5%) is projected for the far future, but a larger increase (50–70%) in strength is projected for all cities during day time. In daily average, about 30% increase in strength is projected for Adelaide and Melbourne, above 20% increase for Brisbane and Canberra, and about 15% increase for Sydney. These changes are statistically significant for all stations except for Sydney.

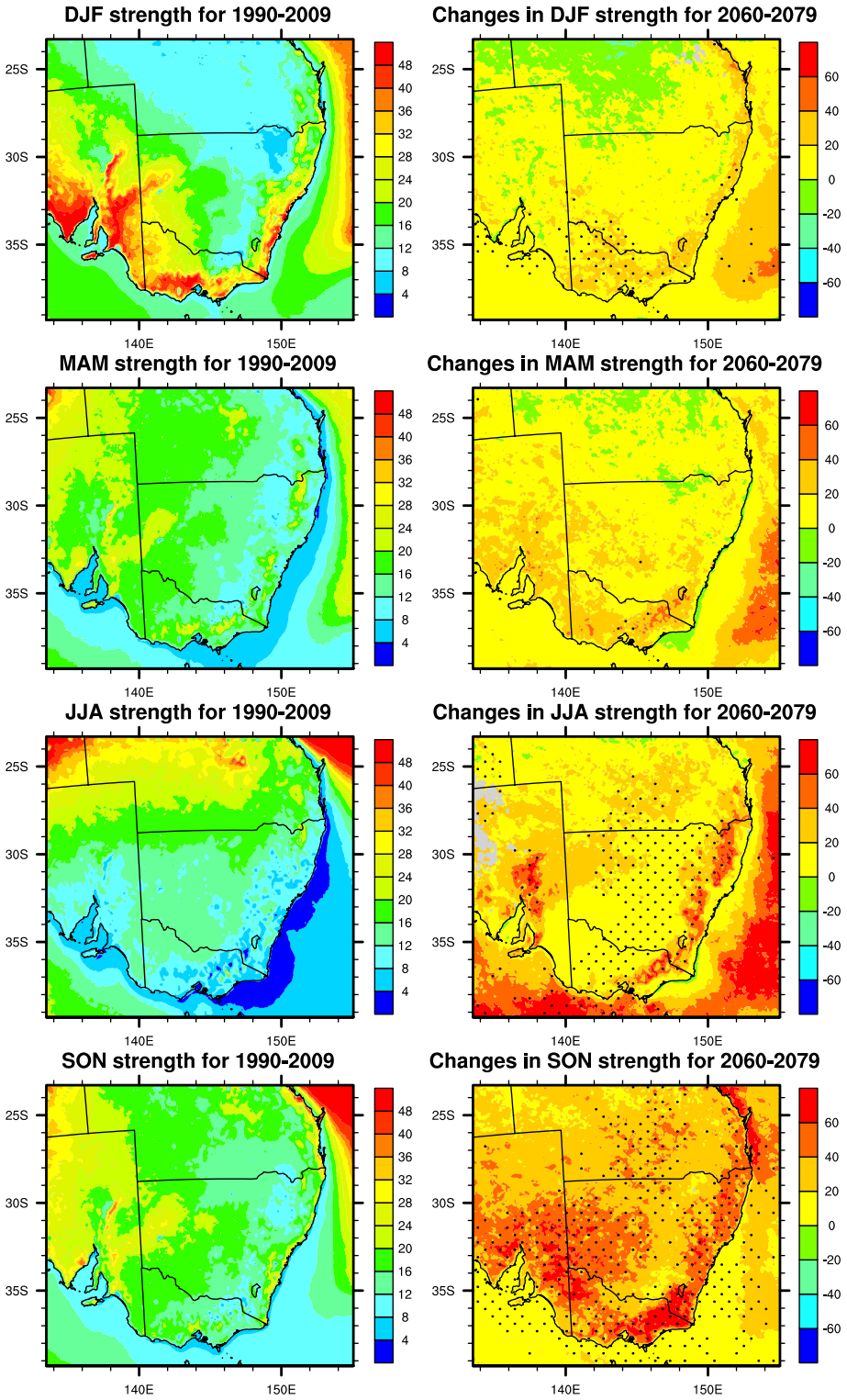

Fig. 4 Seasonal strength of near surface inversions for 1990–2009 (°C/km) and relative changes in strength for 2060–2079 relative to 1990–2009 (%). Stippling and grey colouring convention as in Fig. 3

4.5 Difference among "same GCM driven /same RCM used simulations"

Differences among "same GCM driven /same RCM used simulations" are presented in Figs. 5 and 6. The larger differences between "same GCM driven /same RCM used simulations" are observed for changes in strength. All "same GCM driven simulations" project an increase for most land areas especially for the Great Dividing Range and Flinders Rangers in South Australia where larger increases are projected, however the change magnitudes

Table 3 3-hourly frequency and changes in frequency for five capital cities (unit: %)

Time periods	Cities	Local time							
		1	4	7	10	13	16	19	22
1990–2009	Brisbane	47.41	58.43	45.77	0.80	0.02	0.13	14.00	32.65
	Sydney	30.84	41.48	39.32	5.87	0.08	0.28	6.52	18.42
	Canberra	44.26	53.38	48.96	10.65	0.45	0.24	19.88	37.72
	Adelaide	46.99	50.79	50.59	9.26	0.20	0.11	7.73	40.09
	Melbourne	37.09	42.02	38.84	9.81	0.32	0.33	7.50	26.44
Relative changes for 2060–2079 relative to 1990–2009	Brisbane	−7.00	−5.27	−4.50	8.99	10.34	−7.74	−12.47	−8.91
	Sydney	−3.36	−2.93	−2.13	−9.07	−1.20	−4.39	2.12	−1.79
	Canberra	−1.24	−1.52	−1.26	−0.97	15.14	7.44	−5.22	−1.65
	Adelaide	4.47	4.16	4.25	−7.49	−22.85	34.22	12.99	6.52
	Melbourne	−1.40	−1.79	−2.09	−14.35	13.21	21.61	−3.91	0.11

Table 4 3-hourly strength (°C/km) and changes in strength (%) for five capital cities

Time periods	Cities	Local time							
		1	4	7	10	13	16	19	22
1990–2009	Brisbane	4.44	4.95	6.26	19.97	22.15	39.49	5.73	4.29
	Sydney	5.53	6.24	7.60	8.73	43.79	61.52	14.54	5.40
	Canberra	6.91	7.03	7.92	7.33	11.91	11.86	3.47	5.92
	Adelaide	7.80	8.03	7.75	7.09	35.24	26.24	7.70	6.89
	Melbourne	6.38	6.71	7.26	8.51	28.86	19.47	4.96	5.34
Relative changes for 2060–2079 relative to 1990–2009	Brisbane	−2.84	−4.31	−1.77	**37.33**	**64.39**	**62.29**	**26.55**	1.83
	Sydney	7.26	3.76	2.56	22.19	**46.09**	24.75	3.09	9.32
	Canberra	2.56	2.87	3.43	19.22	**64.87**	**80.47**	10.14	2.86
	Adelaide	10.52	9.78	9.22	**39.32**	**68.74**	**57.69**	16.59	12.92
	Melbourne	6.95	7.58	8.98	**46.13**	**53.11**	**46.29**	**40.94**	9.05

Significant changes are highlighted in bold

are quite different with the largest changes for ECHAM5 driven simulations (central panels in Fig. 5).

Changes in mean strength of near surface inversions projected by the 3 "same RCM used simulations" are similar (central panels in Fig. 6). All RCMs project a more than 30% increase in strength over Great Dividing Range and Flinders Rangers in South Australia, and a more than 10% increase in strength over other land areas except for a small decrease over small areas close to the northern boundary. As there are only 3 and 4 simulations for a "same GCM driven simulation" and "same RCM used simulation", it is not possible to analyze model significance/agreement as in Fig. 3.

"Same GCM driven/same RCM used simulations" generally show similar patterns for changes in inversion characteristics except for strength. Larger differences are observed between "same GCM driven simulations" than "same RCM used simulations". This suggests that large-scale circulation plays a critical role in determining the strength of low level temperature inversions.

4.6 Other inversion characteristics

In this paper, we focused on frequency, strength and duration of near surface temperature inversions. However, other inversion characteristics such as base height of inversion, inversion depths and temperature differences between inversion top and base are also critical to local air quality. Lower base height will lead to pollutants confined in a shallow vertical layer which will increase the concentration of pollutants near the surface. The depth of an inversion layer and difference between its top and bottom determine strength of an inversion. The inversion strength and duration control air quality level. Larger strength usually results in worse air quality.

The results indicate that base heights of inversions generally decrease for majority of land areas. The decreases in base heights of inversions are significant agreeing for most land areas (top panel in Fig. 7). The depth of inversion is projected to increase over land areas especially for the high topography areas, however increases in inversion depth are

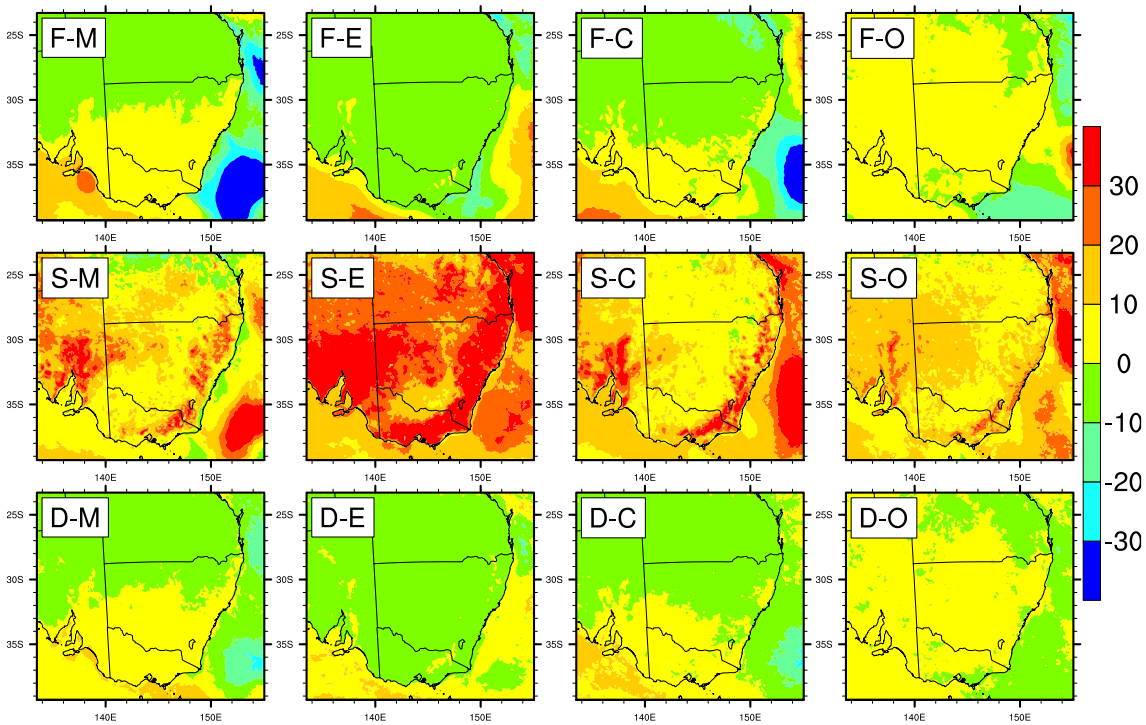

Fig. 5 Mean changes in frequency, strength and duration of near surface inversions for 2060–2079 relative to 1990–2009 for 4 GCM simulations (%). F, S, and D refer to frequency, strength, and duration of temperature inversion, respectively. M, E, C and O refer to MIROC3.2, ECHAM5, CCCMA3.1 and CSIRO-MK3.0 GCMs individually. As there are only three simulations for each "GCM" simulation, which is impractical to analyse model agreement as Fig. 3

only significant for southern land areas (central panel in Fig. 7). Increases in temperature differences between inversion top and base are mostly observed for the southern land areas and these increases are significant (bottom panel in Fig. 7). The strength of inversion shown in Fig. 3 is an average of strength for all inversion events, so the mean changes in temperature difference and changes in inversion depth shown in Fig. 7 cannot directly explain which is critical to projected changes in strength.

5 Discussion

In the evaluation of simulations, R3 is much worse than R1 and R2 in capturing near surface inversion frequency (Fig. 2). As discussed in the Sect. 4.1, the YSU scheme used in R3, which is non-local mixing PBL, is the major cause. However, there is not much difference between R3 and the other two simulations in terms of future changes (Fig. 6). This provides us confidence in future changes for all simulations including those using R3.

Evaluations also show simulations overestimate strength for day time inversion and underestimate strength for night time inversion. As discussed in Sect. 4.1, simulation is not compared at the same time as the observation, this could partly explain the biases in simulations. Furthermore, if there is any systematic bias in simulations, the bias will have minor impacts on future changes in strength (in %) (Di Luca et al. 2017). This is like large frequency biases in R3 simulations shown in Fig. 2, but there is not much difference for the future changes simulated by R3 when compared to other two simulations (Fig. 6). Future changes in strength are larger (more than 40% for daily average shown in Fig. 3 and more than 60% for day time inversion shown in Table 4) and most of these larger changes are statistically significant. These provide us confidence in projected changes in strength.

The simulations projected slight increase (decrease) in frequency and duration for southern (northern) land areas and substantial increase in strength everywhere (Fig. 3). The difference in future projection of near surface inversions between southern and northern areas are mostly due to changes in future regional climate conditions.

A warmer world does not favor near surface inversions, which can be seen in simulations for 1990–2009 (higher frequency in winter and lower in summer in Fig S5 and longer duration in winter and shorter duration in summer in Fig S6). The NARCliM simulations projected much warmer conditions for the northern areas and slightly warmer condition for the southern areas (Olson et al. 2016), which can explain the decrease in frequency and duration for the northern domain

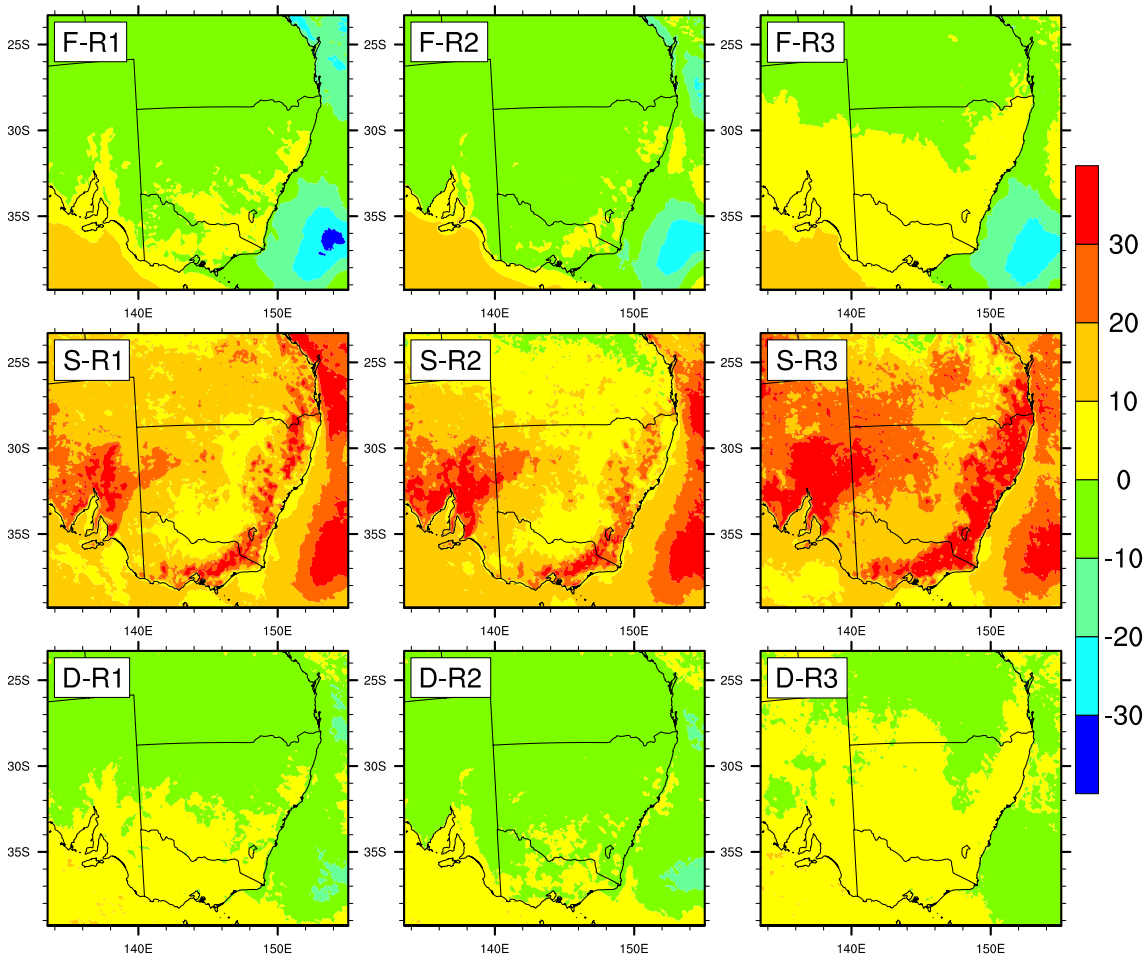

Fig. 6 Mean changes in near surface inversions for 2060–2079 relative to 1990–2009 for 3 RCM simulations (%). F, S, and D refer to frequency, strength, and duration of temperature inversion, respectively. As there are only four simulations for each "RCM" simulation, which is impractical to analyse model agreement as Fig. 3

(Fig. 2). Humidity is one of many factors that contribute to the formation of an inversion. Drier air is easier to cool down than wetter air. The NARCliM simulations projected wetter change for the northern domain, and much drier change for the southern domain especially in winter and spring (Olson et al. 2016), which can explain increase in frequency and duration for the southern areas.

The positive changes in strength of near surface inversions is mostly contributed by larger increase in strength for day time inversion (Fig S4). Near surface inversion is usually stronger during day than in the night, which can be seen in simulations (Fig S3) and observation (Fig. 2). To understand how inversion strength will change in future, we extract temperature difference, inversion depth for each of near surface inversion for land area and analyze correlations among temperature difference, inversion depth and inversion strength.

We group all inversions into various buckets. We set 8 categories for inversion depth (< 200, 200–400, 400–600, 600–800, 800–1000, 1000–1200, 1200–1400, and 1400-1600m), 8 categories for temperature difference (< 2, 2–4, 4–6, 6–8, 8–10, 10–12, 12–14, and 14–16 °C), and 11 categories for inversion strength (< 0.005, 0.005–0.01, 0.01–0.02, 0.02–0.03, 0.03–0.04, 0.04–0.05, 0.05–0.06, 0.06–0.07, 0.07–0.08, 0.08–0.09, and 0.09–0.10 °C/m), then we count number of inversions in each bucket such as temperature difference between 4 and 6 °C, and inversion depth between 400–600m for the historical and future periods. After that, we compare the differences for each bucket between future and historical periods. The results (Fig. 8, Fig S7 and Fig S8) indicate that there is a decrease in the number of weak, "shallow" inversions and an increase in stronger, deeper inversions over the whole land area. This shows that the increases in strength are due to substantial increases in temperature difference.

Investigating this further, we extract temperature profiles for two domains (one in the northern land area and another in the southern land area), each with 900 grids (30 by 30).

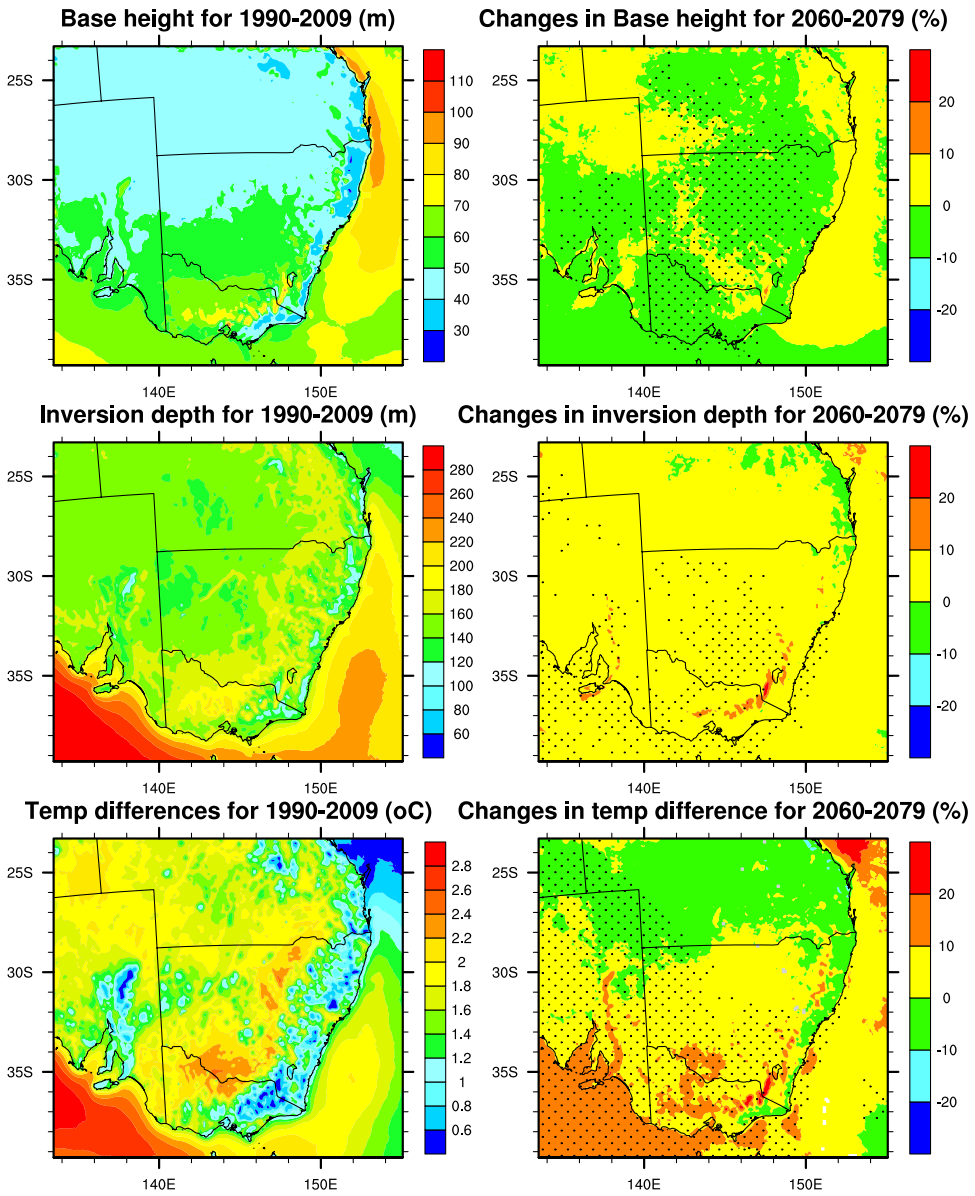

Fig. 7 Mean near surface inversions (units: meter for bottom height and depth, degree for temperature difference) and changes in near surface inversions for 2060–2079 relative to 1990–2009 (unit: %)

Temperature difference (degree)	200	400	600	800	1000	1200	1400	1600
16	0	104	-15	-26	-7	0	0	0
14	64	522	423	234	-49	-2	0	0
12	199	2033	646	903	81	-15	0	0
10	354	2029	2648	1175	29	38	13	0
8	559	617	7616	1990	1028	135	82	-4
6	2154	9674	11229	3745	1003	76	101	-34
4	7343	8483	13650	1715	1052	106	184	33
2	-2160	-3717	1463	-108	190	-11	26	0

Inversion depth (m)

Fig. 8 Changes in number of inversions for temperature difference and inversion depth buckets for 2060–2079 relative to 1990–2009

We calculate mean temperature profiles across 900 grids and 12 ensemble members for historical and future periods. We also calculate mean temperature profiles for inversion events. The difference in temperature profiles between future and historical periods shows that surface warming is substantially less at times when inversions occur compared to the mean warming (Fig S9). This difference between inversion times and the mean decreases as you move up in the atmosphere, disappearing at ~ 750 m height in the southern part of the domain but persisting to ~ 1.5 km in the northern part of the domain. These anomalously cool near surface temperatures lead to an exaggeration of the temperature difference within an inversion. The cause of this cooler surface temperatures is a focus of future research.

Frequency and duration are strongly controlled by the diurnal cycle with most occurring through the night (Fig. S1 and Fig. 3) and the changes looking quite small whether considering "same GCM driven simulations" or "same RCM used simulations". The exception is an increase in frequency in the afternoon which is due to small frequency for 1990–2009. Changes in strength however occur dominantly in the afternoon demonstrate a sensitivity to both the large-scale circulation (difference between "same GCM driven simulations") and the RCM parameterizations especially the PBL scheme.

From the results for "same GCM driven simulations" and "same RCM used simulations", we can see that strength of inversions between "same RCM used simulations" is similar, however, those between "same GCM driven simulations" are quite different in magnitude (Fig S10). This is understandable as GCMs selected in the NARCliM project were chosen based on a number of criteria that includes spanning the range of future changes in the GCM ensemble (Evans et al. 2014). For Australia, MIROC3.2 projects a slightly warmer and much wetter future, CCCMA3.1 extremely warmer and slightly wetter, CSIRO-MK3.0 slightly warmer and drier, and ECHAM5 projected an extremely warmer and slightly drier future. The differences in temperature and humidity projected by 4 GCMs results in diverse change in strength magnitude for four "same GCM used simulations" in Fig. 5. This is consistent with the findings from the previous uncertainty studies, which suggests that the largest uncertainty in future projections is sourced from GCMs (Chen et al. 2011; Teng et al. 2012, Vaze et al. 2011).

There are diverse types of temperature inversions as described in the introduction section. The different inversions are associated with different synoptic conditions. Jiang et al. (2015) used the NARCliM outputs to investigate possible changes in synoptic-scale circulation patterns over southeast Australia in response to global climate change. They found that there are clear differences in simulating synoptic types between different GCM driven simulations. The actual differences of changes in inversion across "GCM simulations" could be related to the difference in simulating synoptic types. Further work is required to analyze future changes for each synoptic type and each inversion group.

The approach to statistical testing used in the study combines testing for significance with the amount of model agreement. Wilks (2016) suggests the area with significant changes in the study might be over-estimated. Future work would be required to combine the False Discovery Rate method with the model agreement framework.

Near surface inversions have substantial impacts on air quality, especially for the larger cities such as the capital cities within the NARCliM domain. Projected results show significant increases in inversion strength for majority of southeast Australia, which will markedly increase pollution levels (Devasthale and Thomas 2012; Wallace et al. 2010). With more than 80% of Australia's population living there and large increases in population projected, the impact of more intense air pollution events in the future could be substantial.

6 Summary and conclusions

The main objective of this paper is to assess how near surface inversions will change under future climate conditions. Firstly, we evaluate the WRF model capability to simulate near surface temperature inversions, then focus the analysis on three temperature inversion characteristics (frequency, strength and duration) and their future projections, seasonal and diurnal variations, and differences between "same GCM driven simulations" and "same RCM used simulations".

Evaluation results indicate that the WRF model captures frequency better than strength of near surface inversions, especially for R1 and R2 simulations, however there is not much difference in projected future changes in inversion characteristics between R3 and other two.

Projected changes in inversion strength are universally positive and significant over the major of southeast Australia, however, changes in frequency and duration are generally small and not significant for most of this region.

There are clear seasonal variations in near surface inversions. Most inversions are in winter and the least in summer, and their duration is longest in winter and shortest in summer. Strength of near surface inversions is also different for the four seasons, but the variation of strength is different from that of frequency and duration.

Inversions have a clear diurnal cycle with higher frequency during night and much lower frequency during day, but strength is generally larger during day than night. This indicates that while few inversions occur during the day, they are usually strong. An increase in strength is projected for all cities especially during day time with a 40–80% increase for different cities. This indicates that there will be stronger

inversions in the future, especially those during day time are projected to get stronger. These could result in an adverse impact on air quality for capital cities.

The differences between "same GCM driven simulations" are larger than those between "same RCM used simulations" only for inversion strength. Four "same GCM driven simulations" projected substantially different magnitude of changes, however three "same RCM used simulations" generally projected similar results in terms of changes in inversion strength. Hence the major uncertainties in projected changes in inversion strength are from using different GCMs.

In conclusion, the results from this study indicate that more near surface inversions with longer duration over the southern land areas, and fewer inversions with shorter duration over the northern land areas, but their strength increases everywhere. This implies that episodes of poor air quality conditions over southeast Australia might become more likely in the future as result of the projected changes in near surface inversions.

Acknowledgements This work is made possible by funding from the NSW Environmental Trust for the ESCCI-ECL project, the NSW Office of Environment and Heritage backed NSW/ACT Regional Climate Modelling Project (NARCliM), and the Australian Research Council as part of the Future Fellowship FT110100576 and Linkage Project LP120200777. Dr. Roman Olson is supported by Basic Science Research Program through the National Research Foundation of Korea (NRF) funded by the Ministry of Science, ICT and future Planning (No. 2014R1A2A1A11049497), and the National Research Foundation of Korea Grant funded by the Korean Government(MEST) (NRF-2009-0093069). The modelling work was undertaken on the NCI high performance computers in Canberra, Australia, which is supported by the Australian Commonwealth Government. We would like to thank Mark Newton for providing the sounding observation for 9 weather stations within the NARCliM domain. This made it possible to evaluate NARCliM simulations in capturing frequency and strength of observed near surface inversions.

References

Abdul-Wahab SA, Bakheit CS, Siddiqui RA (2005) Study the relationship between the health effects and characterization of thermal inversions in the Sultanate of Oman. Atmos Environ 39:5466–5471. https://doi.org/10.1016/j.atmosenv.2005.05.038

AIHW, Begg S, Vos T, Barker B, Stevenson C, Stanley L, Lopez A 2007. The burden of disease and injury in Australia 2003. Cat. no. PHE 82. Canberra: AIHW. <http://www.aihw.gov.au/publication-detail/?id=6442467990>. Viewed 6 Jun 2017

Bailey A, Chase TN, Cassano JJ, Noone D (2011) Changing temperature inversion characteristics in the U.S. southwest and relationships to large-scale atmospheric circulation. J Appl Meteorol Climatol 50:1307–1323. https://doi.org/10.1175/2011JAMC2584.1

Beard JD, Beck C, Graham R, Packham SC, Traphagan M, Giles RT, Morgan JG (2012) Winter temperature inversion and emergency department visits for asthma in Salt Lake County, Uta, 2003–2008. Environ Health Perspect 120(10):1385–1390. https://doi.org/10.1289/ehp.1104349

Bei NF, Xiao B, Meng N, Feng T (2016a) Critical role of meteorological conditions in a persistent haze episode in the Guanzhong basin, China. Sci Total Environ 550:273–284. https://doi.org/10.1016/j.scitotenv.2015.12.159

Bei NF, Li GH, Huang RJ, Cao JJ, Meng N, Feng T, Liu SX, Zhang T, Zhang Q, Molina LT (2016b) Typical synoptic situations and their impacts on the wintertime air pollution in the Guanzhong basin, China. Atmos Chem Phys. 16 7373–7387. https://doi.org/10.5194/acp-16-7373-2016

Bourne SM, Bhatt US, Zhang J, Thomand R (2010) Surface-based temperature inversions in Alaska from a climate perspective. Atmos Res 95(2–3):P353–P366. https://doi.org/10.1016/j.atmosres.2009.09.013

Caserini S, Giani P, Cacciamani C, Ozgen S, Lonati G (2017) Influence of climate change on the frequency of daytime temperature inversions and stagnation events in the Po Valley: historical trend and future projections. Atmos Res 184:15–23

Chen J, Brissette FP, Poulin A, Leconte R (2011) Overall uncertainty study of the hydrological impacts of climate change for a Canadian watershed. Water Resour Res 47:W12509

Chen K, Glonek G, Hansen A, Williams S, Tuke J, Salter A, Bi P (2016) The effects of air pollution on asthma hospital admissions in Adelaide, South Australia, 2003–2013: time-series and case-crossover analyses. Clin Exp Allergy 46:1416–1430. https://doi.org/10.1111/cea.12795

Cohen AE, Cavallo SM, Coniglio MC, Brooks HE (2015) A review of planetary boundary layer parameterization scheme and their sensitivity in simulating southeastern U.S. cold season server weather environments. Weather Forecast 30:591–612. https://doi.org/10.1175/WAF-D-14-00105.1

Connolley W. M. (1996). The Antarctic temperature inversion. Int J Climatol, 16(12):1333–1342. doi:https://doi.org/10.1002/(SICI)1097-0088(199612)16:12<1333::AID-JOC96>3.0.CO;2-6

Czarnecka M, Nidzgorska-Lencewicz J, Rawicki K (2016) Thermal inversions and sulphur dioxide concentrations in some polish cities in the winter season. J Elementol 21:1001–1015. https://doi.org/10.5601/jelem.2016.21.1.1038

Devasthale A, Thomas MA (2012) An investigation of statistical link between inversion strength and carbon monoxide over Scandinavia in winter using AIRS data. Atmos Environ. 56:109–114. https://doi.org/10.1016/j.atmosenv.2012.03.042

Di Luca A, Evans JP, Ji F, 2017. Australian snowpack in the NARCliM ensemble: evaluation, bias correction and future projections. Clim Dyn. https://doi.org/10.1007/s00382-017-3946-9

Evans JP, Ekstrom M, Ji F (2012) Evaluating the performance of a WRF physics ensemble over South-East Australia. Clim Dyn 39:1241–1258. https://doi.org/10.1007/s00382-011-1244-5

Evans JP, Ji F, Abramowitz G, Ekstrom M (2013a) Optimally choosing small ensemble members to produce robust climate simulations. Environ Res Lett 8:044050. https://doi.org/10.1088/1748-9326/8/4/044050

Evans JP, Fita L, Argüeso D, Liu Y (2013b) Initial NARCliM evaluation. In: Piantadosi J, Anderssen RS, Boland J (eds) MODSIM2013, 20th international congress on modelling and simulation. Modelling and Simulation Society of Australia and New Zealand, December 2013, pp. 2765–2771

Evans JP, Ji F, Lee C, Smith P, Argüeso D, Fita L (2014) Design of a regional climate modelling projection ensemble experiment—NARCliM. Geosci Model Dev 7(2):621–629. https://doi.org/10.5194/gmd-7-621-2014

Evans JP, Argueso D, Olson R, Di Luca A, 2016. Bias-corrected regional climate projections of extreme rainfall in south-east Australia. Theor Appl Climatol. https://doi.org/10.1007/s00704-016-1949-9

Feng X, Li Q, Zhu YJ, Wang JJ, Liang HM, Xu RF (2014) Formation and dominant factors of haze pollution over Beijing and its

peripheral areas in winter. Atmos Pollution Res 5:528–538. https://doi.org/10.5094/APR.2014.062

Fita L, Evans JP, Argüeso D, Liu Y (2016) Evaluation of the regional climate response in Australia to large-scale climate modes in the historical NARCliM simulations. Clim Dyn. https://doi.org/10.1007/s00382-016-3484-x

Hou P, Wu SL (2016) Long-term changes in extreme air pollution meteorology and the implications for air quality. Sci Rep. https://doi.org/10.1038/srep23792

Ji F, Ekstrom M, Evans JP, Teng J (2014) Evaluating rainfall patterns using physics scheme ensembles from a regional atmospheric model. Theoret Appl Climatol 115:297–304. https://doi.org/10.1007/s00704-013-0904-2

Ji F, Evans JP, Scorgie Y, Jiang N, Argüeso D, Di Luca A (2015) Change in frequency, intensity and duration of temperature inversion for southeast Australia, MODSIM2015, Gold Coast, Australia, Nov 29–Dec 4, 2015

Ji F, Evans JP, Teng J, Scorgie Y, Argüeso D, Di Luca A (2016) Evaluation of long-term precipitation and temperature WRF simulations for southeast Australia. Clim Res 67:99–115. https://doi.org/10.3354/cr01366

Jiang NB, Ji F, Di Luca A, Scorgie Y, Riley M, Evans JP (2015) Changes in synoptic circulation patterns associated with projected future climate. AMOS National Conference, July 15–17, 2015, Brisbane

Kahl JD (1990) Characteristics of the low-level temperature inversion along the Alaskan Arctic coast. Int J Climatol 10(5):P537–P548. https://doi.org/10.1002/joc.3370100509

Kahl JD, Serreze MC, Schnell RC (1992) Tropospheric low level temperature inversion in the Canadian Arctic. Atmos Ocean 30(4):P511-P529. https://doi.org/10.1080/07055900.1992.9649453

Kalnay E et al. (1996) The NCEP/NCAR 40-year reanalysis project. Bull Am Meteorol Soc 77:437–470

Kassomenos PA, Koletsis IG (2005) Seasonal variation of the temperature inversions over Athens, Greece. Int J Climatol 25(12:1651–1663. https://doi.org/10.1002/joc.1188

Kusaka H, Kondo H, Kikegawa Y, Kimura F (2001) A simple single-layer urban canopy model for atmospheric models: comparison with multi-layer and slab models. Bound Layer Meteorol 101:329–358. https://doi.org/10.1023/A:1019207923078

Largeron Y, Staquet C (2016) The atmospheric boundary layer during wintertime persistent inversions in the Grenoble valleys. Front Earth Sci. https://doi.org/10.3389/feart.2016.00070

Milionis AE, Davies TD (2008) A comparison of temperature inversion statistics at a coastal and a non-coastal location influenced by the same synoptic regime. Theor Appl Climatol 94:225–239. https://doi.org/10.1007/s00704-007-0356-7

Nodzu MI, Ogino SY, Tachibana Y, Yamanaka MD (2006) Climatological description of seasonal variations in lower-tropospheric temperature inversion layers over the Indochina Peninsula. J Clim 19(13):3307–3319. https://doi.org/10.1175/JCLI3792.1

Olson R, Evans JP, Luca Di A, Argueso D (2016) The NARCliM project: model agreement and significance of climate projections. Clim Res 69(3):209–227. https://doi.org/10.3354/cr01403

Pietroni I, Argentini S, Petenko I (2014) One year of surface-based temperature inversions at dome C, Antarctica. Bound Layer Meteorol 150(1):131–151, https://doi.org/10.1007/s10546-013-9861-7

Rendón AM, Salazar JF, Palacio CA, and Wirth V., and Brötz B (2014) Effects of urbanization on the temperature inversion breakup in a mountain valley with implications for air quality. J Appl Meteor Climatol 53:840–858. https://doi.org/10.1175/JAMC-D-13-0165.1

Skamarock WC, Klemp JB, Dudhia J, Gill DO, Barker DM, Duda MG, Huang XY, Wang W, Powers JG (2008) A description of the advanced research WRF Version 3, NCAR technical note. NCAR, Boulder

Tebaldi C, Arblaster JM, Knutti R (2011) Mapping model agreement on future climate projections. Geophys Res Lett 38:L23701. https://doi.org/10.1029/2011GL049863

Teng J, Vaze J, Chiew FHS, Wang B, Perraud J-M (2012) Estimating the relative uncertainties sourced from GCMs and hydrological models in modeling climate change impact on runoff. J Hydrometeorol 13(1):122–139

Tomasi C. (1977) Precipitable water vapor in atmospheres characterized by temperature inversions. J Appl Meteor 16:237–243. https://doi.org/10.1175/1520-0450(1977)016<0237:PWVIAC>2.0.CO;2

VanReken TM, Dhammapala RS, Jobson BT, Bottenus CL, VanderSchelden GS, Kaspari SD, Gao ZM, Zhu RQ, Lamb BK, Liu HP, Johnston J (2017) Role of persistent low-level clouds in mitigating air quality impacts of wintertime cold pool conditions. Atmos Environ 154:236–246. https://doi.org/10.1016/j.atmosenv.2017.01.043

Vaze J, Teng J, FHS Chiew (2011) Assessment of GCM simulations of annual and seasonal rainfall and daily rainfall distribution across south-east Australia. Hydrol Process 25(9):1486–1497. https://doi.org/10.1002/hyp.7916

Wallace J, Corr D, Kanaroglou P (2010) Topographic and spatial impacts of temperature inversions on air quality using mobile air pollution surveys. Sci Total Environ 408:5086–5096. https://doi.org/10.1016/j.scitotenv.2010.06.020

Wang SYS, Hipps LE, Chung OY, Gillies RR, Martin R (2015) Long-term winter inversion properties in a mountain valley of the western United States and implications on air quality. J Appl Meteorol Climatol 54:2339–2352. https://doi.org/10.1175/JAMC-D-15-0172.1

Wang S, Liao TT, Wang LL, Sun Y (2016) Process analysis of characteristics of the boundary layer during a heavy haze pollution episode in an inland megacity, China. J Environ Sci 40:129–144. https://doi.org/10.1016/j.jes.2015.12.008

Whiteman C. D, Bian XD, and Zhong SY (1999) Wintertime evolution of the temperature inversion in the Colorado plateau basin. J Appl Meteorol 38, 1103–1117. https://doi.org/10.1175/1520-0450(1999)038<1103:WEOTTI>2.0.CO;2

Whiteman CD, Hoch SW, Horel JD, Charland A (2014) Relationship between particulate air pollution and meteorological variables in Utah's Salt Lake Valley. Atmos Environ 94:742–753. https://doi.org/10.1016/j.atmosenv.2014.06.012

Wilks DS (2016) The Stippling shows statistically significant grid points. BAMS. https://doi.org/10.1175/BAMS-D-15-00267.1

Zora JE, Sarnat SE, Raysoni AU, Johnson BA, Li WW, Greenwald R, Holguin F, Stock TH, Sarnat JA (2013) Associations between urban air pollution and pediatric asthma control in El Paso, Texas. Sci Total Environ 448:56–65. https://doi.org/10.1016/j.scitotenv.2012.11.067